Effect of Perfluorooctane Sulfonate on the Renal Cortex of Adult Male Albino Rats and the Possible Ameliorating Role of Quercetin

Original Article

Mohammed Ahmed Shehata Amin and Rasha Ahmed Agaga

Department of Human Anatomy and Embyology, Faculty of Medicine, Zagazig University, Egypt.

ABSTRACT

Introduction: Perfluorinated chemicals (PFCs) are materials that have many important industrial applications. Quercetin is a unique bioflavonoid that known with its antioxidant activity.

Aim: To evaluate the histopathological effect of (PFOS) on rat renal cortex and the possible protective role of Quercetin.

Materials and Methods: 45 adult male albino rats were divided into three groups, each contained 15 rats. The first group was the control group (I), which was splitted into three equal subgroups. The second group was (PFOS) receiving group (II) at a dose of 20mg /kg/day by gavage for 28 days. The third group was the protective group (III) which received the same dose of (PFOS) as group (II) in combination with Quercetin at a dose of 50 mg/kg b.w orally for 28 days. At the end of the study, the kidneys were dissected out and prepared for light microscopic examination.

Results: The kidney sections of (PFOS) receiving group showed distortion of normal histology in the form of variations in the size and shape of renal glomeruli, peri glomerular inflammatory cell infiltrations, Disorganized renal tubules with dark stained (pyknotic) nuclei, cystic luminal dilatation and cytoplasmic vacuolations. In addition, some cortical convoluted tubules showed areas of interstitial hemorrhage, necrosis and exfoliation of tubular epithelial cells. Increased collagen fibers deposition and immune expression of PCNA and INOS stained sections. All these findings were improved by co-administration of Quercetin.

Conclusion: Quercetin played an important role in improving the toxic effects of (PFOS) on kidney tissue of adult male rats.

Key Words: Kidney, perfluorooctane Sulfonate, quercetin.

Revised: 27 March 2022, **Accepted:** 5 May 2022.

Corresponding Author: Mohammed Ahmed Shehata Amin, MD, Department of Human Anatomy and Embyology, Faculty of Medicine, Zagazig University, Egypt, **Tel.:** 00201223769469, **E-mail:** dr.mohammed.shehata2007@gmail.com

ISSN: 2536-9172, December 2022, Vol. 6, No. 2

INTRODUCTION

Perfluorinated chemicals (PFCs) are substances with unique criteria that known to have numerous important manufacturing and engineering applications. Although these materials have been widely used in the last century, concerns about the environmental dangers of these compounds arose only newly, and researches regarding human and animals exposure are increasing[1]. There is a growing alarm concerning human exposure to (PFCs), including perfluorooctanoic acid (PFOA) and perfluorooctane sulfonate (PFOS), because these chemicals are constant in the environment, bio-accumulated, and biomagnified along food chains and have been shown to cause developmental and other undesirable health effects in experimental animals. PFCs have been extensively used in the manufacture of industrial and consumer products for example waterproof surfactants, lubricants, polishes, paper and clothes coatings, food packaging, and fire-fighting foams used for distinguishing fires near airports and military bases[2, 3]. Per- and polyfluoroalkyl substances (PFASs) have been found in earth, air, and water from all regions of the world, as a result, (PFASs) are now accepted as worldwide ubiquitous toxicants[4]. Humans are intoxicated through ingestion of polluted soil, food, and water, and inhalation of polluted air. Noticeable levels are found in the majority of humans, and in the US, nearly all adults have established some level of PFAS exposure[5]. Even with efforts to decrease or remove production, the drinking water for six million US inhabitants still exceeds the lifetime health recommendations for both (PFOS) and (PFOA)[6]. PFASs are increasingly associated with carcinogenesis, disturbance of endocrine, metabolic and immunologic pathways, reproductive and developmental toxicity[7]. Elevated levels of (PFOS) and (PFOA) were detected in the kidneys, as they are the main route for PFCs elimination[8]. Additionally, rats exposed to PFOS showed renal hypertrophy and histological changes, indicating involvement of soft tissue proliferation in the renal parenchyma and renal microvascular disease[9]. Quercetin is a distinctive bioflavonoid that has been broadly discussed by researchers over the last 30 years. Flavonoids belong to a group of normal substances with variable phenolic structure and are present in the fruits, vegetables, grains, bark roots, stem, flowers, tea and wine[10]. Quercetin is considered to be a potent antioxidant

 DOI: 10.21608/jmh.2022.129889.1097

owing to its ability to scavenge free radicals and bind transition metal ions. These criteria of Quercetin allow it to prevent lipid peroxidation. Lipid peroxidation can produce harmful effects all over the body, for example cardiovascular and neurological diseases; on the other hand, it can be eliminated by antioxidants, as Quercetin, which interferes by reacting with the radicals formed. Quercetin can also minimize inflammation by scavenging free radicals. Free radicals can stimulate transcription factors that generate proinflammatory cytokines, which are frequently present, elevated in patients that have chronic inflammatory diseases[11]. So the present study aimed to shed light on the toxic effect of Perfluorooctane Sulfonate (PFOS) and the possible protective role of Quercetin on the kidney structure of adult male albino rats.

MATERIALS AND METHODS

Animals and experimental design:

45 Wister adult male albino rats weighing 200-250 g were obtained from Animal House, Faculty of Medicine, Zagazig University, Egypt. Ethical approval was obtained from the animal care committee of the National Research Center (IACUC), Zagazig University, Egypt, the approval number was (ZU-IACUC/3/F/14/2021). All animals were subjected to 1 week of passive preliminaries in order to adapt themselves to their new environment and to ascertain their physical wellbeing. They were housed in separate well ventilated cages, under standard conditions, with free access to food and water ad libtium. The experiment was performed at the Animal House of Faculty of Medicine, Zagazig University. The rats were classified into three groups, each contained 15 rats. The first group was the control group (I), which was splitted into three equal subgroups, 5 rats per each. Subgroup Ia (control –ve) in which rats received only regular diet and distillated water for 28 days. Subgroup Ib (vehicle subgroup) where rats received Milli-Q water (vehicle for PFOS) 1 ml/kg /day for 28 days[12]. Subgroup Ic (control +ve) was the Quercetin administered group at a dose of 50 mg/ kg b.w orally for 28 days. The second group was (PFOS) receiving group (II), in which a solution of PFOS was administrated daily by diluting the PFOS in Milli-Q water at a dose of 20mg / kg/day by gavage for 28 days. The concentration of PFOS was (0.5 mg/mL) as described by[12]. The third group was the protective group (III) which received the same dose of (PFOS) for the same period as group (II) in combination with Quercetin at a dose of 50 mg/ kg b.w orally for 28 days. At the end of the study, all rats were anaesthetized and sacrificed using intraperitoneal injection of thiopental 50 mg/kg[13]. Midline laparotomy was performed; both kidneys were dissected out and processed for light microscopic examination.

Histological Study:

Each kidney was cut into two halves across the renal pelvis along its longitudinal axis to expose cortex, medulla and papilla. Samples of the renal tissue were kept frozen in dry ice and subsequently stored at −80°C. The renal tissue samples were fixed in 10% formalin and embedded in paraffin. Serial 5-µm sections were prepared from the paraffin embedded samples of all the studied groups and the sections were stained with hematoxylin and eosin (H&E)[14] and Masson trichrome staining to clarify histological details and the presence of collagen fibers around renal tubules and renal glomeruli respectively. The sections were examined under a LEICA research microscope (LEICA Dm750, Switzerland) at Human Anatomy department, Zagazig university with a digital camera attached (LEICA ICC50). Digital photomicrographs of stained sections were taken.

Biochemical study:

Venous blood samples were taken from animals by capillary glass tubes from the retro-orbital plexus as described by[15]. About 2 ml of blood was allowed to perculate into a centrifuge tube, and incubated at 37ºC until blood clotted then centrifuged to separate the serum. The samples were maintained at (-20°C) to be used for estimation of creatinine and blood urea nitrogen in the serum using a commercially available spectrophotometric enzymatic kit (Thermo Trace BECGMAN, Germany).

Immuno-histochemical evaluation:

For the immunohistochemical studies, paraffin sections were deparaffinized in xylene and processed for inducible nitric oxide synthase (iNOS), and Proliferating cell nuclear antigen (PCNA) immunohistochemical study. Immunohistochemistry was performed using a three-step indirect process based on the labeled avidin-biotin peroxidase complex (ABC) method. Sections were rehydrated in descending grades of alcohol. Following blocking of endogenous peroxidase activity with 3% H2O2 in methanol and non-specific binding sites with a protein blocker, the sections were incubated for 32 min with a 1:100 dilution of iNOS (rabbit anti-rats iNOS polyclonal antibody, Santa Cruz Biotechnology, Santa Cruz, CA, USA) and PCNA (rabbit monoclonal, Novus Biologicals, Abingdon, UK) primary antibodies. Next, a biotinylated secondary antibody was added at a concentration of 2% for 30 min (37°C) followed by the addition of the ABC. Visualization of the reaction was performed using 3, 3'-diaminobenzidine (DAB) as the chromogen, which produces a dark brown precipitate that is readily detected by light microscopy. The sections were then counterstained with Mayer's hematoxylin, dehydrated in ascending grades of alcohol, cleared in xylene, and mounted with distyrene (a polystyrene), a plasticizer (tricresyl phosphate), and

xylene. iNOS cytoplasmic and nuclear reaction sites stained brown; whereas the PCNA immunoreactions were indicated by brown coloration in nuclei of renal cells. The negative control included sections that were incubated in the absence of iNOS, and PCNA primary antibodies[16].

Morphometry and image analysis:

Image analysis and morphometry was performed by using Image J software (Wayne Rasband, National Institute of Mental Health, Bethesda, Maryland, USA). Mean area percentage of collagen fibers deposition was determined in sections stained by Masson trichrome stain at x400 magnification. As well as, sections marked by PCNA antibody, the mean area percentages of immune positive nuclei were assessed. In addition, apoptosis was quantified by measuring the mean area percentage of iNOS positive cells in each field within ten non-overlapping fields at x400 magnification.

STATISTICAL ANALYSIS

The data was analyzed by using one-way ANOVA followed by the Tukey's post-hoc multiple range test. Different variables were shown as mean ± SD and a value of $P < 0.05$ was considered significant. All statistical analysis was performed by using SPSS statistical version 15.

RESULTS

Histological Study:

Light microscopic examination:

1. Hematoxylin and eosin stain (H&E):

H&E stained sections of the control subgroups 1a, 1b and 1c of adult male renal cortex showed no histological variations between the three subgroups. Thus, the findings of subgroup 1a were chosen to illustrate the control group, which appeared as thin renal capsule surrounding the renal cortex (RC). The (RC) is formed of (Malpighian) renal corpuscles and tubules. Each renal corpuscle was made up of a tuft of capillaries (the glomerulus) surrounded by visceral and parietal layers of Bowman's capsule that separated from each other by Bowman's space. The outer parietal layer formed of flat cells whereas the inner visceral layer is closely related to glomerular capillaries. The renal tubules formed mainly of proximal and distal convoluted tubules. The proximal convoluted tubules were lined with cuboidal epithelial cells with eosinophilic cytoplasm and central rounded nuclei, and the distal convoluted tubules were lined with a relatively large number of cuboidal epithelial cells. The lumens of the distal tubules were wider than those of the proximal tubules; their cytoplasm was less acidophilic; and the nuclei were round as shown in (Figure 1). In (PFOS) administered group, sever destructive changes of renal cortex were seen when compared with control groups. Some glomeruli were hypertrophied with narrow or absent Bowman's space (BS), glomerular hypercellularity and congested capillaries. Other glomeruli appeared atrophied with wide (BS), while others were lobulated. In some areas, peri glomerular inflammatory cell infiltrations were observed. Disorganized renal tubules with dark stained (pyknotic) nuclei, cystic luminal dilatation, cytoplasmic vacuolations and detachment of some tubular epithelial cells within the lumens were noticed. In addition, some cortical convoluted tubules showed deposition of homogenous acidophilic materials in their lumens, areas of interstitial hemorrhage, necrosis and exfoliation of tubular epithelial cells were observed as shown in (Figure 2). Considering protective (III) group, a variable degree of improvement was identified when compared with (PFOS) administered group. The renal cortex was enclosed by a relatively thin renal capsule, and apparently normal glomeruli were surrounded by visceral and parietal layers of Bowman's capsule with nearly normal Bowman's space. Some cortical convoluted tubules were still demonstrating vacuolation in their cells, while other proximal and distal convoluted tubules began to restore their normal histological construction. Somewhat, few hypertrophied renal glomeruli with nearly obliterated Bowman's space can be seen as shown in (Figure 3).

2. Masson's trichrome stain:

Masson's trichrome-stained sections of the control subgroups showed few green coloured collagen fibers in the renal glomeruli and in the renal interstitium surrounding the renal tubules and blood vessels. Few dense green coloured collagen fibers around glomerular capillaries within the glomeruli were also observed as shown in (Figure D). In (PFOS) administered group, abundant green coloured collagen fibers were noticed in the interstitium around blood vessels, renal tubules and glomeruli. In addition, extensively green coloured collagen fibers around the glomerular capillaries were seen as shown in (Figure E). Considering protective (III) group, Masson's trichrome stained sections showed moderate amounts of green coloured collagen fibers in the renal interstitium around renal tubules, blood vessels and glomerulus. Moderately dense green coloured collagen fibers around glomerular capillaries were also observed as shown in (Figure F).

3. Immunohistochemical-staining with PCNA:

The immunohistochemical stained sections of the control subgroups showed few numbers of PCNA-positive nuclear immunoreactions in both glomerular and renal tubular cells as shown in figure (G). In (PFOS) administered group, the immunohistochemical-stained sections revealed marked increase in the number of PCNA-positive nuclear glomerular and renal tubular cells in comparison to the relevant control group as shown in (Figure H). Regarding the protective (III) group, the immunohistochemical-

stained sections showed marked decrease in the number of PCNA-positive nuclear glomerular and renal tubular cells in comparison to the (PFOS) administered group as shown in (Figure I).

4. Immunohistochemical-staining with iNOS:

The immunohistochemical stained sections of the control subgroups showed a weak iNOS immune-positive reaction in the glomeruli but an immune-negative reaction in the proximal and distal convoluted tubules as shown in (Figure J). In (PFOS) administered group, the immunohistochemical-stained sections revealed mild iNOS immune-positive reactions in the glomeruli and marked reactions in most of the proximal and distal convoluted tubules as shown in (Figure K). Regarding the protective (III) group, the immunohistochemical-stained sections showed weak iNOS immune-positive reactions in most of the glomeruli, the proximal and distal convoluted tubules as shown in (Figure L).

5. Morphometric Study and Statistical Analysis:

Considering masson trichrome stained sections, the results of the present study showed that the area percentage of collagen fibers was increased in group (II) when compared to group (I). It was significantly decreased in group (III) when compared to group (II), but still significantly higher than group (I) as shown in (Table 1). As regards iNOS immunohistochemical stained sections, The area percentage of immune reaction to iNOS was increased in group (II) when compared to group (I) .It was significantly decreased in group (III) when compared to group (II), but still significantly higher than group (I) as shown in (Table 2). Regarding PCNA immunohistochemical stained sections, the number of immune positive nuclei to PCNA was increased in group (II) when compared to group (I).It was significantly decreased in group (III) when compared to group (II). There was no significant difference between group (I) and group (III) as shown in (Table 3) and (Figure 7).

6. Biochemical Study and Statistical Analysis:

The results of the present study showed a very highly significant increase in serum activities of Creatinine and BUN ($p < 0.001$) in the PFOS receiving group when compared with control group and highly significant increase ($p < 0.01$) when compared with protective group as shown in (Table 4) and (Figure 8).

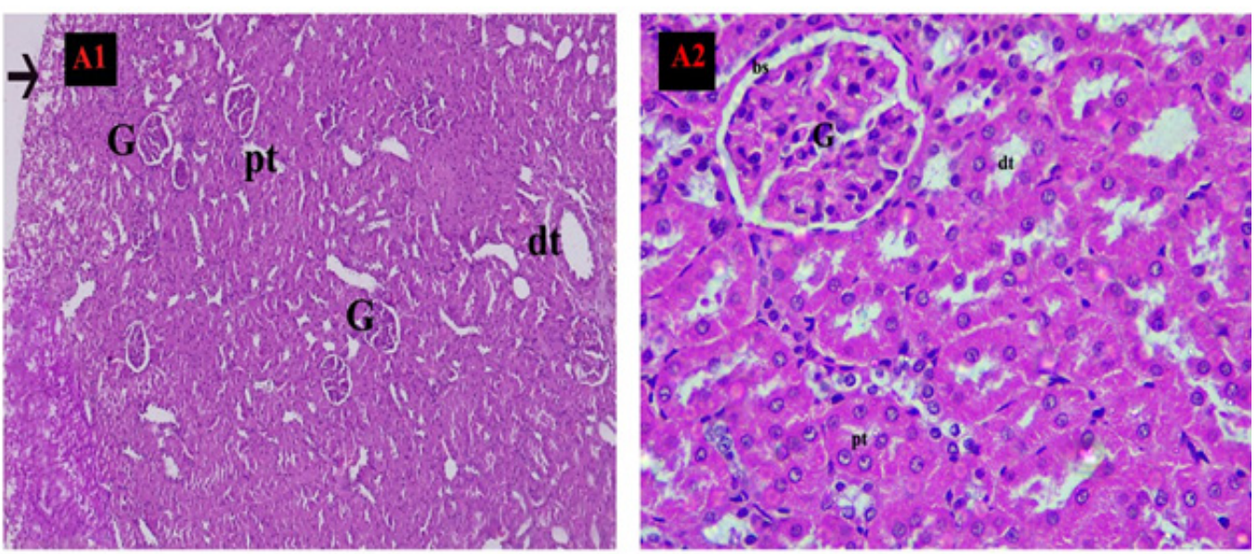

Fig. 1: (A1) A photomicrograph of a section from the renal cortex of a control adult male albino rat showing normal renal glomeruli (G), proximal tubules (pt) and distal tubules (dt).Thin renal capsule (arrow) is clearly defined. (H&E ×100). (A2) showing a renal corpuscle consisting of a glomerulus (G) and Bowman's space (bs). The proximal convoluted tubules (pt) are lined by a single layer of tall cubical cells with narrow lumens while the distal convoluted tubules (dt) with wide lumens are clearly defined. (H&E ×400).

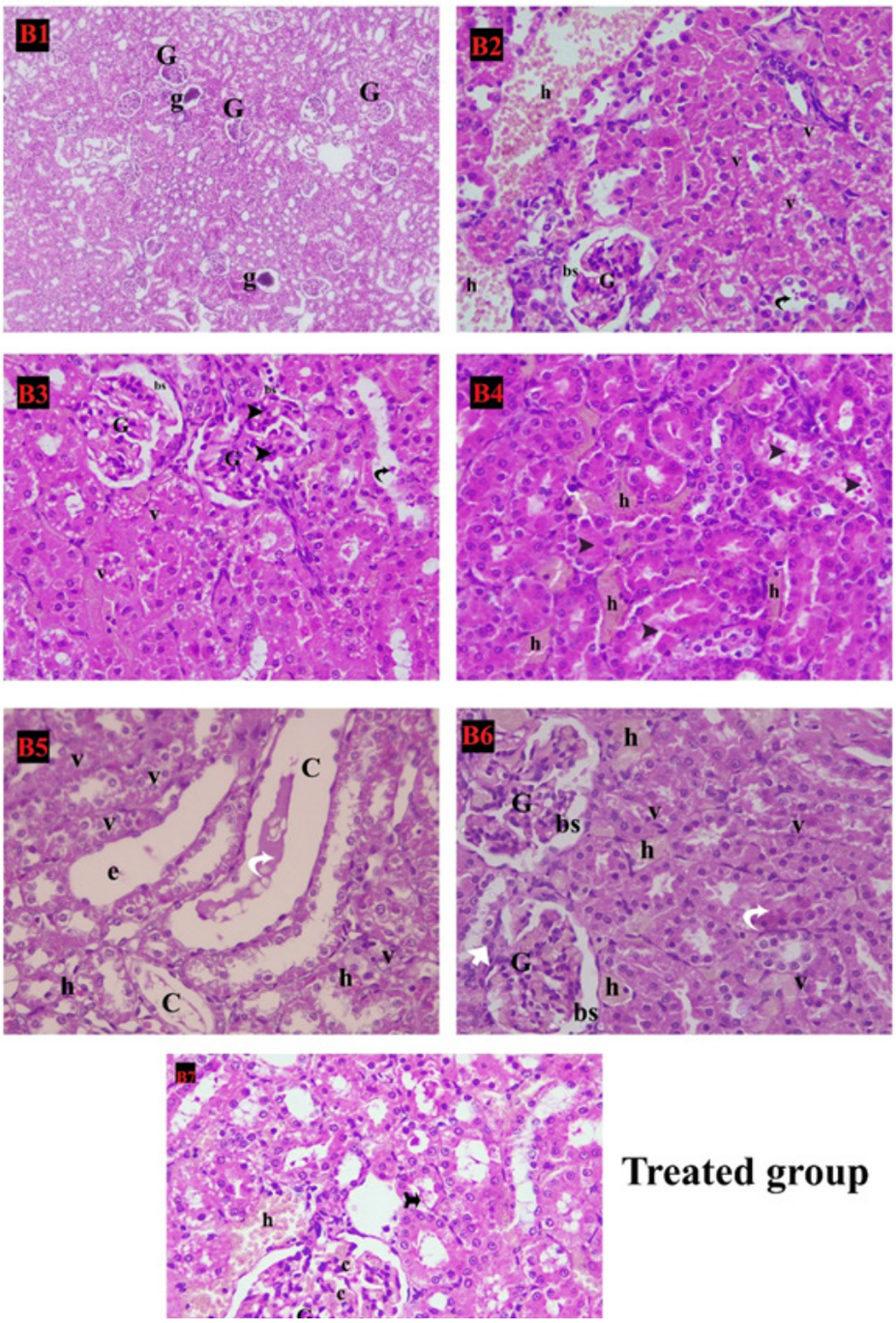

Fig. 2: (B1) A photomicrograph of a section from the renal cortex of adult male albino rat treated with PFOS showing hypertrophied glomerulus (G) with narrow or obliterated Bowman's space. Other glomeruli (g) are atrophied and shrunken with wide Bowman's space. (H&E ×100). (B2) showing lobulated glomerulus (G) with widened Bowman's space (bs) .Multiple vacuolizations (v) of the tubular cytoplasm. Exfoliated nuclei into the lumen of tubules (curved arrow) and large areas of interstitial hemorrhage (h) are also observed. (H&E ×400). (B3) showing hyper-cellularity of the glomerulus (G) with proliferation of mesengial cells (arrow head) obliterating Bowman's space (bs). Another glomerulus is lobulated with widened Bowman's space (bs). Exfoliated nuclei into the lumen of tubules (curved arrow). Multiple vacuolizations (v) of the tubular cytoplasm are present. (H&E ×400). (B4) showing multiple areas of interstitial hemorrhage (h) and Homogenous acidophilic material (arrow head) in the tubular lumen. (H&E ×400). (B5) showing disorganized renal tubules with cystic luminal dilatation (C), necrosis of tubular epithelial lining and exfoliation of cells in their lumens (e). Homogenous acidophilic material in the tubular lumen (white curved arrow), areas of hemorrhage (h) and multiple vacuolations (V) are noticed. (H&E ×400). (B6) showing lobulated glomerulus (G) with widened Bowman's space (bs). Inflammatory cellular infiltrations (arrow head) are present on the side the glomerulus. Multiple vacuolizations (v) of the tubular cytoplasm, homogenous acidophilic material into the tubular lumen (curved white arrow) and multiple areas of interstitial hemorrhage (h) are also observed. (H&E ×400). (B7) showing hypertrophied glomerulus (G) with dilated congested capillaries (c). Homogenous acidophilic material (tailed arrow) in the tubular lumen and area of hemorrhage (h) are also observed. (H&E ×400).

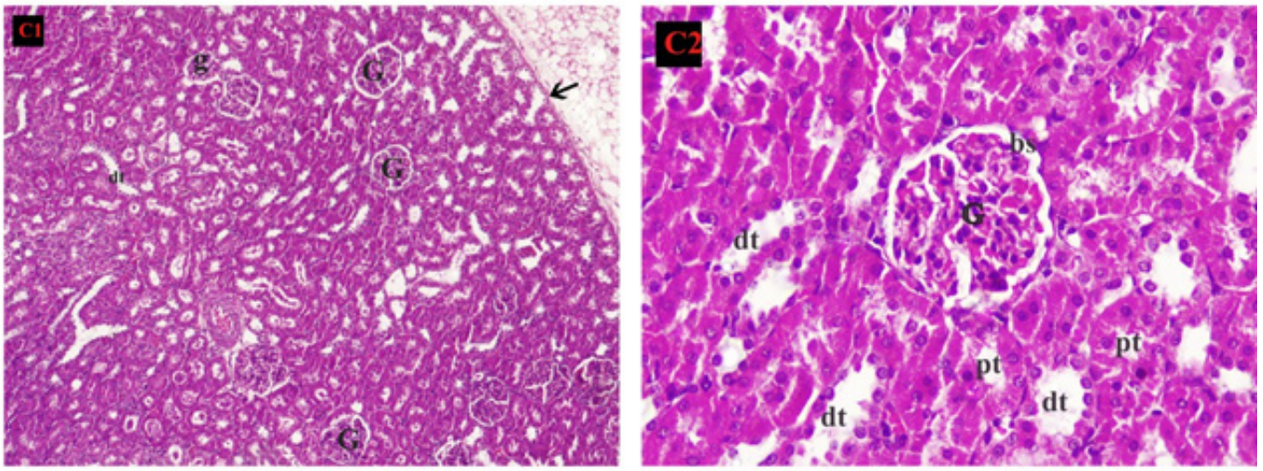

Fig. 3: (C1) A photomicrograph of a section of the kidney of an adult male albino rat (treated with PFOS+ Quercetin) showing intact renal capsule (arrow). The renal cortex is formed mainly of normal renal corpuscles (G), few shrunken glomerulus (g) and normal distal convoluted tubules (dt). (H&E × 100). (C2) Showing a renal corpuscle consisting of an apparently normal glomerulus (G) and Bowman's space (bs). The proximal convoluted tubules (pt) are lined by a single layer of normally tall cubical cells with narrow lumens. The lumens of the distal convoluted tubules (dt) are wider and clearly defined than the proximal tubules. (H&E ×400).

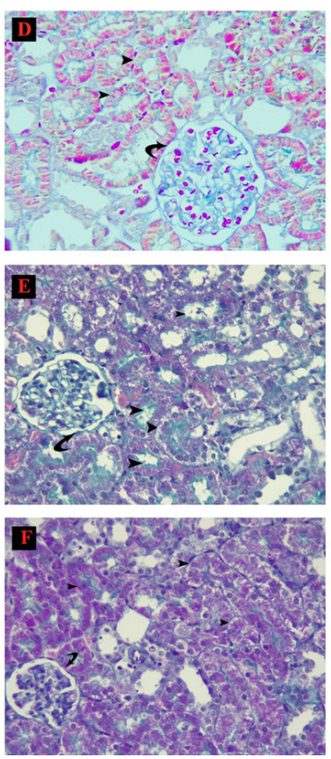

Fig.4: (D) A photomicrograph of a section of kidney of control adult male albino rat showing few green coloured collagen fibers in the renal interstitium (arrow head) surrounding the renal tubules. Few green coloured collagen fibers around renal glomeruli (curved arrow) were also observed. (E) A section of kidney treated with PFOS of adult male albino rat showing abundant green coloured collagen fibers located around renal tubules (arrow head) and renal glomeruli (curved arrow). In addition, extensively green coloured collagen fibers around glomerular capillaries are noticed within Glomeruli. (F) A section of kidney treated with PFOS+ Quercetin of adult male albino rat showing moderate amounts of green coloured collagen fibers in the renal interstitium around renal tubules (arrow head) and glomeruli (curved arrow). Moderately dense green coloured collagen fibers around glomerular capillaries were also observed. (Masson's trichrome x400).

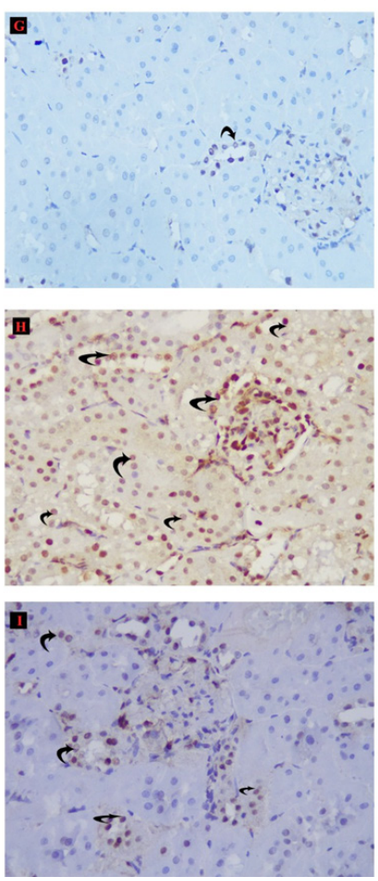

Fig. 5: (G) A Photomicrograph of kidney section of control adult male albino rat showing few numbers of PCNA-positive nuclear immunoreactions (curved arrow). (H) A kidney section treated with PFOS of adult male albino rat showing marked increase in the number of PCNA-positive nuclear glomerular and renal tubular cells (curved arrow) in comparison to the relevant control group. (I) A section of kidney treated with PFOS+ Quercetin of adult male albino rat showing marked decrease in the number of PCNA-positive nuclear glomerular and renal tubular cells(curved arrow) in comparison to the (PFOS) administered group. (PCNA IHC X400).

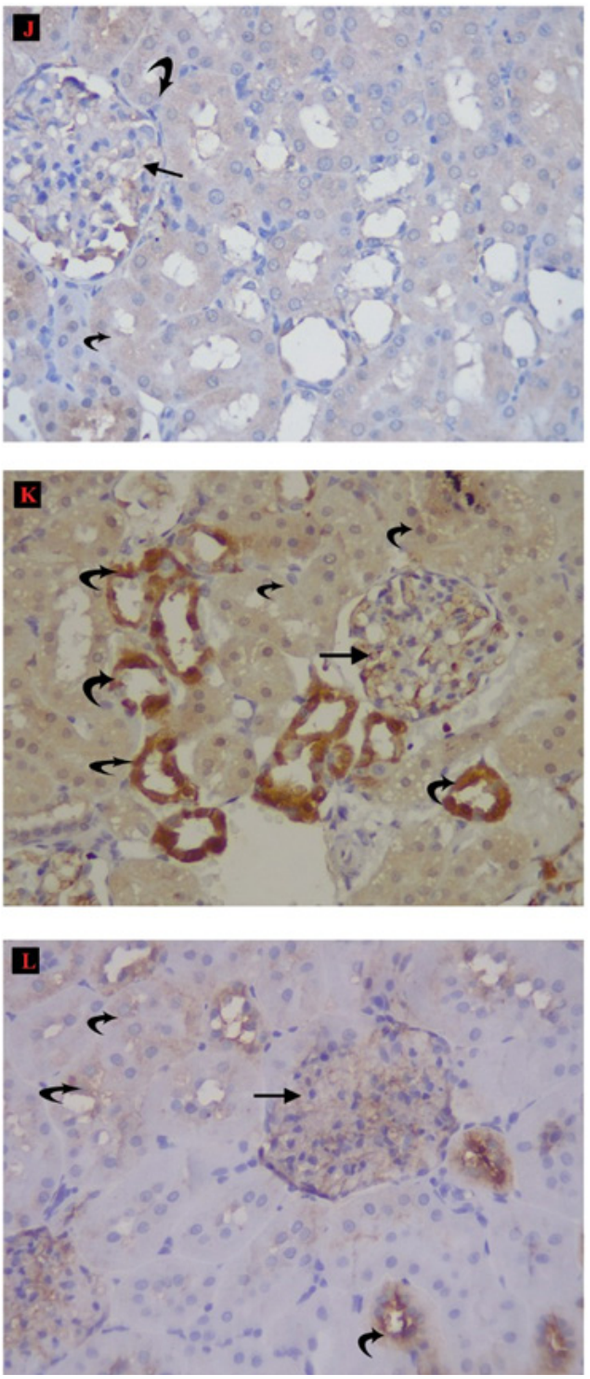

Fig. 6: (J) A photomicrograph of a section of kidney of control adult male albino rat showing a weak positive iNOS immune reaction in the glomeruli (arrow) but an immune-negative reaction in the proximal and distal convoluted tubules (curved arrow). (K) Section treated with PFOS of adult male albino rat showing mild iNOS immune-positive reactions in the glomeruli (arrow) and marked reactions in most of the proximal and distal convoluted tubules(curved arrow). (L) Section of kidney treated with PFOS+ Quercetin of adult male albino rat showing weak iNOS immune-positive reactions in the glomerulus (arrow) and most of the proximal and distal convoluted tubules (curved arrow). (iNOS IHC X400).

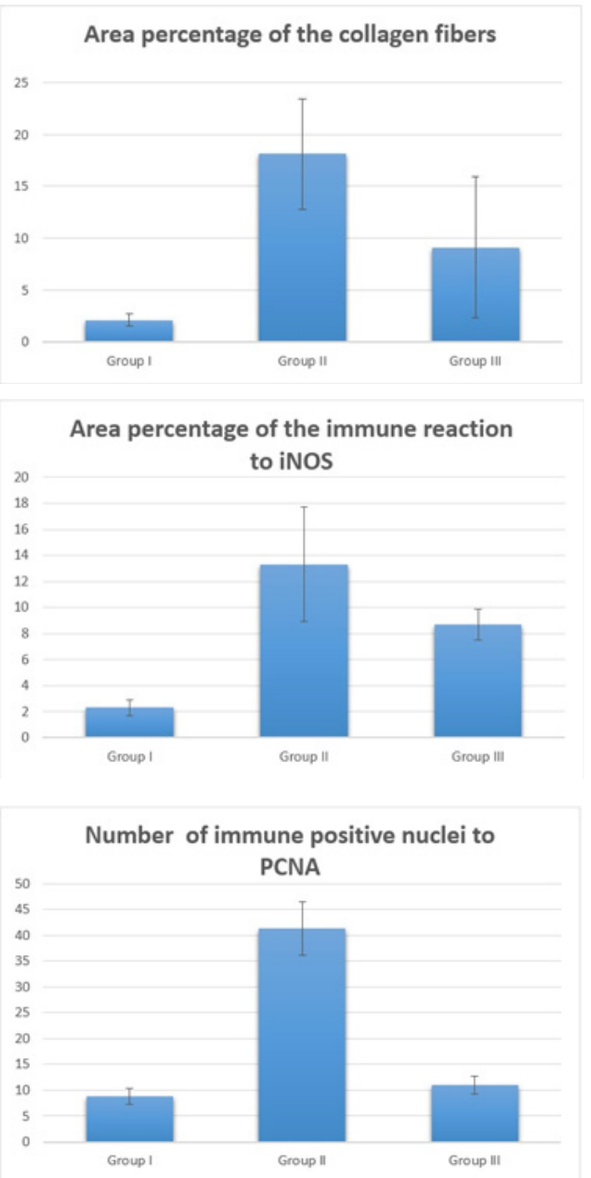

Fig. 7: A Histogram demonstrating the effects of PFOS and Quercetin on different morphometrical parameters in the renal cortex of adult male rats including (area percentages of collagen fibers, area percentages of the immune reaction to iNOS and number of immune positive nuclei to PCNA) in the different studied groups.

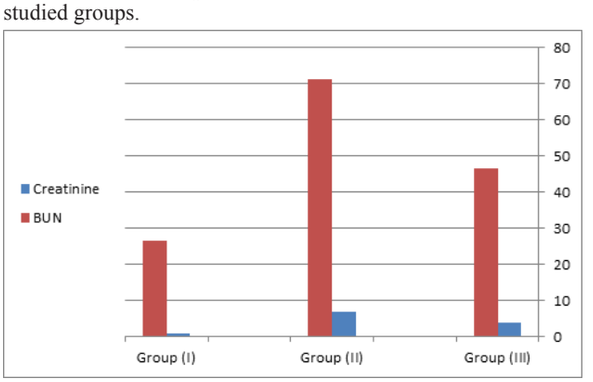

Fig. 8: A Histogram demonstrating the effects of PFOS and Quercetin on Creatinine & BUN in the different studied groups.

Table 1: Statistical analysis of area percentage of collagen fibers in the different groups

Group / Parameter	Group I	Group II	Group III	F	*P*
Area percentage of the collagen fibers	2.1 ± 0.6	18.1[a] ± 0.9	9.1[ab] ± 1.7	452.9	*<0.001***

a: significant from group I
b: significant from group II
**: highly significant one-way ANOVA test

Table 2: Statistical analysis of area percentage of immune reaction to iNOS in the different groups.

Group / Parameter	Group I	Group II	Group III	F	*P*
Area percentage of immune reaction to iNOS	2.3 ± 0.6	13.3[a] ± 4.4	8.7[ab] ± 1.2	42.3	*<0.001***

- Data represent mean ± SD
a: significant from group I
b: significant from group II
**: highly significant one-way ANOVA test

Table 3: Statistical analysis of number of immune positive nuclei to PCNA in the different groups.

Group / Parameter	Group I	Group II	Group III	F	*P*
The number of immune positive nuclei to PCNA	8.8 ± 1.5	41.3[a] ± 5.1	11[b] ± 1.8	318.4	*<0.001***

- Data represent mean ± SD
a: significant from group I
b: significant from group II
**: highly significant one-way ANOVA test

Table 4: Comparisons between mean values of serum creatinine and BUN in the different studied groups using ANOVA (analysis of variance) test.

Groups / Parameter	Group (1) Control (n=15)	Group (II) PFOS (n=15)	Group (III) Protective (n=15)	F	*P*
Creatinine mg/dL Mean± Sd	0.98 ± 0.17	6.96 ± 1.32	3.74 ± 0.74	40.94	*< 0.001****
BUN mg/dL Mean± Sd	26.5 ± 9.31	71.2 ± 6.97	46.5 ± 4.74	44.11	*< 0.001****

*** Very highly significant n= number of rats of each group=15
Sd: Standard deviation

DISCUSSION

Perfluoroalkyl and polyfluoroalkyl substances (PFAS), or sometimes called Perfluorinated compounds (PFCs), a class of environmentally persistent and bioaccumulative contaminants, including perfluorooctane sulfonate (PFOS), perfluorooctanoic acid (PFOA), and perfluorododecanoic acid, have been found in the environment. As emerging contaminants, PFAS can reach the water, atmosphere, soil, sludge, and other environmental media by all routes, and they have caused widespread pollution[9].

Consequently, in this study, considerable attention has been paid to the potential toxicity of PFOS, one of the members of the PFAS, because the environmental hazard caused by this compound is very dangerous specially to the kidney.

PFOS induced oxidative stress not only by increasing the activation of NADPH oxidase but also by eliminating the induction of antioxidant enzymes (i.e., Gpx-1, SOD-1, and catalase)[17].

Histopathological observations have indicated that greater concentrations of PFOS and PFOA were found in the kidneys[8, 18] because they are the primary route of PFC excretion[19].

Several lines of recent proof have suggested that an association between PFOA and PFOS and CKD may be possible, including evidence for renal hypertrophy and histopathological changes indicative of soft tissue proliferation in the renal interstitium and renal microvascular disease in rats exposed to PFCs[9] and the effect of PFCs in increasing endothelial cell permeability[20, 21], which is a mechanism of renal injury in rat models of ischemic renal failure[22–23].

The mechanisms through which PFOS produces developmental toxicity remain unclear. Furthermore, one possible toxicity mechanism underlying PFOS exposure has been reported to alter mitochondrial biogenetics[24, 3].

Quercetin (QE) has been demonstrated to possess a broad range of physiological neuroprotective, anti-inflammatory, antioxidant, antiapoptotic, antigenotoxic and anticarcinogenic activities[25, 26].

Zou *et al*., (2015)[27] who reported that QE-treatment inhibited the production of oxidative stress biomarkers MDA, hydrogen peroxide, and 8-hydroxy-2'-deoxyguanosine, reduced the levels of proinflammatory cytokines interleukin 6, cyclooxygenase-2 and C-reactive protein in the PFOA-treated mice.

The renal histopathological findings in the present study showed distorted renal tubules in the form of cystic luminal dilatation, pyknosis, necrosis, detached epithelial cells and deposition of homogenous acidophilic material (cast) into the tubular lumens as a result of PFOS intoxication. However, these histological findings were ameliorated by Quercetin administration.

Deposition of homogenous acidophilic hyaline material observed in the present work, was in agreement with Hegazy *et al*., (2016)[28] who reported that the treated animals showed intraluminal and intracytoplamic accumulation of hyaline droplets and renal cast.

Concerning the renal glomeruli in the present work, there were variable forms of pathological damage in the form of shrinkage, atrophy, lobulation and hypertrophy of renal glomeruli, glomerular hypercellularity, congestion of glomerular capillaries and widening or obliteration of Bowman's space. The shrinkage and atrophy of renal glomeruli that were observed in this work were in consistence with Soudani *et al*., (2010)[29] who established shrunken glomerulus with widening of bowman's space. Also, Hegazy *et al*., (2016)[28] documented the same results in their study as well as thickening of glomerular basement membrane.

Mayer, (2003)[30] explained the correlation between tubular interstitial nephritis and glomerular injury as tubular damage linked with tubular obliteration influence the flow of glomerular filtrate. If the glomerular filtration rate was slowed or stopped, glomerular shrinkage and sclerosis occurred. Moreover, Apostolova *et al*., (2005)[31] and L'Azou *et al*., (2007)[32] attributed the glomerular shrinkage to the disruption of the cytoskeleton of the mesengial cells and their contraction.

Also, in accordance with Hanan *et al*., (2010)[33] who recorded dilatation of Bowman's space, shrinkage of glomeruli and dilatation of both proximal and distal convoluted tubules in the kidney of animals treated with gibberellic acid for 50 days. Moreover, Samir *et al*., (2012)[34] found that increased intertubular spaces and dilatation of tubules became due to renal tubular atrophy.

For vacuolar formation found here in the present study, similar findings were proved before by Sakr *et al*., (2003)[35], where they demonstrated that vacuolization in cytoplasm is one of the important earlier responses to all forms of cell injury. They explained that by increased permeability of cell membranes leading to an increase of intracellular water. So water sufficiently accumulates within cells producing cytoplasmic vacuolization.

The above mentioned results obtained also by Zahid *et al*., (2007)[36] who reported that the lesion in the renal corpuscles appeared in the form of a hydropic change or swelling with cytoplasmic vacuolization in the parietal cells of the Bowman’s capsule.

Fartkhooni *et al*., (2016)[37] in their study also reported swelling and dilatation of Bowman's capsule. Also, Altayeb *et al*., (2017)[38] documented several renal histopathological changes associated with dilated congested glomerular capillaries. Regarding renal tubules, some were degenerated with numerous tubular dilation and most of their lumens contained homogenous acidophilic cellular debris. Some tubular cells appeared with dark stained pyknotic nuclei while others showed cytoplasmic degeneration or vacuolations in consistent with Altayeb *et al*., (2017)[38] who revealed changes as; flattening of the epithelial lining of some tubules, exfoliation and pyknosis of some tubular cells with apparent luminal dilatation and intratubular cell debris.

Fartkhooni *et al*., (2016)[37] also reported deposition of hyaline- like materials in some proximal tubules and degenerative changes in epithelial lining of the proximal tubules as a result of titanium nanoparticles toxicity.

In this study, Masson's trichrome stained sections of control group showed few collagen fibers in the renal interstitium around renal corpuscles and tubules. These results are close to those of Hassan & Mazher, (2011)[39].

While, Masson's trichrome stained sections of treated group revealed histological changes and areas of interstitial fibrosis appear as segmental and global glomerular sclerosis and tubule-interstitial injury in the form of tubular dilatation and atrophy of tubular epithelial cells. The same result occurred with gibberellic acid effect on the kidney according to Hanan *et al*., (2010)[33].

Helmy *et al*., (2015)[40] referred that to the interstitial fibrosis as an end stage of the sequelae of fluid oozing outside the tubules, edema and cellular infiltrations. However, they pointed out that fibroblasts may be transformed from the flattened cells, with their flattened nuclei, lining some tubules. The lesion that occurred in the renal corpuscles in the treated group could be attributed to peritubular fibrosis and it was in agreement with that seen by Abdel-Rahman *et al*., (2017)[41].

Moawad *et al*., (2019)[42] described this lesion as 'cystic glomerular atrophy' based on the small size of some glomeruli within the dilated Bowman's space.

Takahashi *et al*., (2005)[43] attributed the pathogenesis of this lesion to periglomerular fibrosis and stated that thickening of glomerular basement membrane resulted in disturbance of glomerular outflow that led to cystic changes in Bowman's space.

But, in the present study, some renal cortical glomeruli of PFOS treated rats exhibited more cellularity. Some authors attributed this due to compensation for the decrease in developing glomeruli with increase in vascular glomeruli firmly filling Bowman capsule[44].

The current study revealed little collagen fibers in the cortical interstitium around the renal corpuscles and tubules in Masson's trichrome stained specimens of protected groups. The results agreed with Ahmed *et al*., (2019)[45].

The (PFOS) administered group in the present study exhibited significant increase of iNOS immunohistochemical reaction. This result was in agreement with those of other studies that demonstrated an increase in iNOS expression as detected by immunohistochemistry in the kidneys of hemorrhagic shock (HS) rat models. Increased expression of iNOS enhances the formation of NO and may contribute to circulatory failure and organ dysfunction associated with HS. In addition, it has been reported that NO promotes apoptosis via activation of c-Jun[16].

Several toxicology studies demonstrated unequivocal histological, cellular, and metabolic kidney-related outcomes related to PFOS exposure, including increased oxidative stress, enhanced apoptosis and fibrosis with tubular epithelial histological changes, and enhanced microvascular endothelial permeability through actin filament remodeling[46].

Regarding PCNA stained sections in the present study, there were marked increase in its expression in the (PFOS) administered group. These findings were confirmed also by morphometric analysis. These results were in consistence with Hassan *et al*., (2020)[47] who examined the toxic effect of gibberellic acid postnatally on renal cortex of albino rats.

The present study reported increased serum levels of creatinine and BUN. This comes in line with Troudi *et al*., (2011)[48] who reported that, levels of creatinine and urea in treated off springs were higher in plasma and lower in urine than those of the control. Moreover, Erin *et al*., (2008)[49] explained the increased urea level due to either the Ammonia increased protein catabolism or the transformation of ammonia to urea. This was in the same line of Sakr *et al*., (2002)[50].

CONCLUSION

Rats exposed to PFOS exhibit nephrotoxic manifestations. Additionally, the use of Quercetin may be beneficial in improving these manifestations being a potent antioxidant.

CONFLICT OF INTEREST

There are no conflicts of interest.

REFERENCES

1. **Houde, M.; Martin, JW.; Letcher, RJ.; Solomon, KR. and Muir, DC. (2006):** Biological

monitoring of polyfluoroalkyl substances: A review. Environmental science & technology. 40(11):3463–3473. PMID: 16786681.

2. **Environmental Protection Agency. (2010):** Perfluorooctanoic Acid (PFOA) and Fluorinated Telomers. Washington, DC: Environmental Protection Agency; (http://www.epa.gov/oppt/pfoa/). (Accessed May 5, 2010).

3. **Lau C, Anitole K, Hodes C, *et al.* (2007):** Perfluoroalkyl acids: a review of monitoring and toxicological findings. Toxicol Sci. 99(2):366–394.

4. **Buck, RC.; Franklin, J.; Berger, U.; Conder, JM.; Cousins, IT.; de Voogt, P.; Jensen, AA.; Kannan, K.; Mabury, SA. and van Leeuwen, SP. (2011):** Perfluoroalkyl and polyfluoroalkyl substances in the environment: Terminology, classification, and origins. Integr Environ Assess Manag, 7: 513– 541.

5. **Calafat, AM.; Wong, LY.; Kuklenyik, Z.; Reidy, JA. and Needham, LL(2007):** Polyfluoroalkyl chemicals in the U.S. population: Data from the National Health and Nutrition Examination Survey (NHANES) 2003-2004 and comparisons with NHANES 1999-2000. Environ Health Perspect, 115: 1596–1602.

6. **Hu, XC.; Andrews, DQ.; Lindstrom, AB.; Bruton, TA.; Schaider, LA.; Grandjean, P.; Lohmann, R.; Carignan, CC.; Blum, A.; Balan, SA.; Higgins, CP. and Sunderland, EM. (2016):** Detection of Poly- and Perfluoroalkyl Substances (PFASs) in U.S. drinking water linked to industrial sites, military fire training areas, and wastewater treatment plants. Environ Sci Technol Lett, 3: 344–350.

7. **Li K, Gao P, Xiang P, Zhang X, Cui X, Ma LQ. (2017):** Molecular mechanisms of PFOA-induced toxicity in animals and humans: Implications for health risks. Environ Int, 99: 43–54.

8. **Han, X.; Kemper, RA. and Jepson, GW. (2005):** Subcellular distribution and protein binding of perfluorooctanoic acid in rat liver and kidney. Drug and chemical toxicology. 28(2):197–209. doi: 10.1081/DCT-52547 PMID: 15865261.

9. **Cui, L.; Zhou, QF.; Liao, CY.; Fu, JJ. and Jiang, GB. (2009):** Studies on the toxicological effects of PFOA and PFOS on rats using histological observation and chemical analysis. Archives of environmental contamination and toxicology. 56(2):338–349. Epub 2008/07/29. doi: 10.1007/s00244-008-9194-6 PMID:18661093.

10. **Middleton EJ. (1998):** Effect of plant flavonoids on immune and inflammatory cell functions. Adv Exp Med Biol; 439:175-182.

11. **Satyendra, SB.; Nikhil, S.; Rajendra, SB.; Preeti, A, Sarlesh, R. (2012):** A review of Quercetin: antioxidant and anticancer Properties. World journal of pharmacy and pharmaceutical sciences. 1, 1, 146-160.

12. **Zhang P, Shi YL, Cai YQ, Mou SF (2007):** Determination of Perfluorinated compounds in water samples by high performance liquid chromatography-electrospray tandem mass spectrometry .Chin J Anal Chem 35:969–972.

13. **Institutional Animal Care and Use Committee (IACUC), Office of Research Compliance (ORC) (2013):** Non-pharmaceutical and Pharmaceutical Grade Compounds in Research Animals.https://research.iu.edu/doc/compliance/animal-care/bloomington/iub-biacuc-non-pharmaceutical-and-pharmaceutical-grade-compounds-in-research-animals.pdf.

14. **Rönn, T.; Lendemans, S.; de Groot, H. and Petrat, F. (2011):** A new model of severe hemorrhagic shock in rats. Comp. Med. 61; 419–426.

15. **Joslin, J. O. (2009):** Blood collection techniques in exotic medicine. Journal of exotic Medicine. 18: 117-139.

16. **Al Drees, A.; Khalil, MS. and Soliman, M. (2017):** Histological and Immunohistochemical Basis of the Effect of Aminoguanidine on Renal Changes Associated with Hemorrhagic Shock in a Rat Model. Acta Histochem. Cytochem. 50 (1): 11–19, doi: 10.1267/ahc.16025

17. **Kennedy GL Jr.; Butenhoff, JL.; Olsen, GW; *et al.* (2004):** The toxicology of perfluorooctanoate. Crit Rev Toxicol. 34(4):351–384.

18. **Yoo, H.; Guruge, KS.; Yamanaka, N.; *et al.* (2009):** Depuration kinetics and tissue disposition of PFOA and PFOS in white leghorn chickens (Gallus gallus) administered by subcutaneous implantation. Ecotoxicol Environ Saf; 72(1):26–36.

19. **Butenhoff, JL.; Kennedy GL Jr.; Hinderliter, PM.; *et al*. (2004):** Pharmacokinetics of perfluorooctanoate in cynomolgus monkeys. Toxicol Sci. 82(2):394–406.

20. **Qian, Y.; Ducatman, A.; Ward, R, *et al*. (2010):** Perfluorooctane sulfonate (PFOS) induces reactive oxygen species (ROS) production in human microvascular endothelial cells: role in endothelial permeability. J Toxicol Environ Health A. 73(12): 819–836.

21. **Hu, W.; Jones, PD.; DeCoen, W, *et al*. (2003):** Alterations in cell membrane properties caused by Perfluorinated compounds. Comp Biochem Physiol C Toxicol Pharmacol. 135(1):77–88.

22. **Sutton, TA.; Fisher, CJ. and Molitoris, BA. (2002):** Microvascular endothelial injury and dysfunction during ischemic acute renal failure. Kidney Int. 62(5):1539–1549.

23. **Sutton TA. (2009);** Alteration of microvascular permeability in acute kidney injury. Microvasc Res. 77(1):4–7.

24. **Bjork JA, Lau C, Chang SC, Butenhoff JL, Wallace KB. (2008):** Perfluorooctane sulfonate-induced changes in fetal rat liver gene expression. Toxicology.; 251(1–3):8–20. doi:10.1016/j.tox.2008.06.007PMID:18692542

25. **Jung, M., Bu, S.Y., Tak, K.H., Park, J.E., and Kim, E. (2013):** Anticarcinogenic effect of quercetin by inhibition of insulin-like growth factor (IGF)-1 signaling in mouse skin cancer, Nutr. Res. Pract. 7 439–445.

26. **Li, M., Jiang, Y., Jing, W., Sun, B., Miao, C., and Ren, L. (2013):** Quercetin provides greater cardioprotective effect than its glycoside derivative rutin on isoproterenol-induced cardiac fibrosis in the rat, Can. J. Physiol. Pharmacol. 91 951–959.

27. **Zou, W., Liu, W., Yang, B., Wu, L., Yang, J., Zou, T., and Zhang, D. (2015):** Quercetin protects against perfluorooctanoic acid-induced liver injury by attenuating oxidative stress and inflammatory response in mice. International immuno-pharmacology, 28(1), 129-135. https://doi.org/10. 1016/j. intimp.2015.05.043

28. **Hegazy, R.; Salama, A.; Mansour, D. and Hassan, A. (2016):** Renoprotective Effect of Lactoferrin against Chromium- Induced Acute Kidney Injury in Rats: Involvement of IL-18 and IGF-1 Inhibition. PloS One., 11 (3): 1-18. DOI: 10.1371/ journal.pone.0151486, 2009.

29. **Soudani, N.; Sefi, M.; Amara, I.B.; Boudawara, T. and Zeghal, N. (2010):** Protective effects of selenium (Se) on chromium (VI) induced nephrotoxicity in adult rats. Ecotoxicology and Environmental Safety, 73 (4): 671678. https://doi.org/10.1016/j.ecoenv.2009.10.002.

30. **Mayer T. (2003):** Tubular injury in renal disease. Kidney International, 63: 774-787. DOI:10.1046 /j.1523-1755.2003.00795.

31. **Apostolova, M.D.; Christova, T. and Templeton, D.M. (2005):** Involvement of gelsolin in cadmium-induced disruption of the mesengial cell cytoskeleton. Toxicological Sciences, 89 (2): 465-474. https://doi.org/10.1093/toxsci/ kfj035.

32. **L'azou, B.; Dubus, I.; Ohayon-Courtès C. and Cambar, J. (2007):** Human glomerular mesangial IP15 cell line as a suitable model for in vitro cadmium cytotoxicity studies. Cell Biology and Toxicology, 23 (4): 267-278, doi: 10.1007/s10565-006-0888-0.

33. **Hanan, A. E. S.; Mona, M. M. and Hany, M. H. (2010):** Biochemical and molecular profiles of gibberellic acid exposed albino rats. Journal of American Science, 11: 18-23.

34. **Samir, A. N.; Fawzya, A.; Ahmed, M. H.; Mohamed, N. M. and Asmaa, S. H. (2012):** Cytogenetic, histological and histochemical studies on the effect of gibberellin A3 in albino rats. Journal of American Science; 8(1) 75-83.

35. **Sakr, S. A.; Okdah, Y. A. and El- Abd, S. (2003):** Gibberellin A3 induced histological and histochemical alterations in the liver of albino rats. Science Asia, 29: 327- 331. Cited from Samir A. Nassar, Fawzya Ab.Zayed, Ahmed M. Hegab, Mohamed N. Mossaad and Asmaa S. Harfoush (2012).

36. **Zahid, M.; Kamal, F.; Qamar, M.Z.; Bhatti, S.A.; and Insari, N.I. (2007):** Morphological changes produced by aminoglycoside induced nephrotoxicity - an experimental study. ANNALS; 13(4): 234-237

37. **Fartkhooni FM, Noori A, and Mohammadi A. (2016):** Effects of titanium dioxide nanoparticles toxicity on the kidney of male rats. International Journal of Life Sciences 10 (1): 65 – 69.

38. **Altayeb, Z.M. El Mahala-way, A.M. and Salem, M.M. (2017):** Histological and Immunohistochemical Study of Titanium Dioxide Nanoparticle Effect on the Rat Renal Cortex and the Possible Protective Role of Lycopen. Egyption Journal of Histology 40(1):80

39. **Hassan, G. M. and Mazher, K. H. M. (2011):** Genotoxicity and .histopathological studies on the liver, kidney and lymphocytes of male rats fed on diet containing waste fat released from chicken during grilling process. Journal of Cytology and Histology, 2(1):1-8.

40. **Helmy AM, Sharaf-El-Din NA, Abd-El-Moneim RA, and Rostom DR (2015):** Histological study of the renal cortical proximal and distal tubules in adult male albino rats following prolonged administration of titanium dioxide nanoparticles and the possible protective role of l-carnosine. The Egyptian Journal of Histology 38:126 -142

41. **Abdel-Rahman MA, Abdel-Atty YH, Abdel-Rahman MM, Sabry M. (2017):** Structural changes induced by gibberellic acid in the renal cortex of adult male albino rats. MOJ AnatPhysiol; 3:21–27.

42. **Moawad RS, El Fattah A, Ramadan E, Ramadan RS. (2019):** Postnatal Effect of Acrylamide on Rat Renal Cortex and The Protective Effect of Ginger (ZingiberOfficinale Roscoe). Egyptian Journal of Histology, 42(1), 51-63.

43. **Takahashi M, Morita T, Sawada M, Uemura T, Haruna A, Shimada, A. (2005):** Glomerulocystic kidney in a domestic dog. J Comp Pathol; 133:205– 208.

44. **Abdel-Mawla A, Ahmed M, HusamEldien O. (2011):** HPLC analysis and role of the Saudi Arabian propolis in improving the pathological changes of kidney treated with monosodium glutamate. Spatula DD; 1:119–127.

45. **Ahmed AOH, Mokhtar HEL, Helmy HOM, Abd El-Fatah SSA. (2019):** Structural Changes Induced by Potassium Dichromate in Renal Cortex of Adult Male Albino Rats and the Possible Protective Role of Selenium. The Medical Journal of Cairo University, 87(March), 661-675. doi:10.21608/mjcu.2019.52521.

46. **Chou, HC.; Wen, LL.; Chang, CC.; Lin, CY.; Jin, L. and Juan, SH. (2017):** From the cover: L-carnitine via PPARg- and Sirt1-dependent mechanisms attenuates epithelial-mesenchymal transition and renal fibrosis caused by perfluorooctane sulfonate. Toxicol Sci 160: 217–229.

47. **Hassan, NH.; Farag, AI. and Mohammed, HO.(2020):** Histological and immunohisto-chemical study of toxic effect of gibberellic acid postnatally on renal cortex of albino rats. Egyptian Journal of Histology, DOI: 10.21608/ejh.2020.21044.1214.

48. **Troudi A, Amara IB, Soudani N, Samet AM, Zeghal N. (2011):** Oxidative stress induced by gibberellic acid on kidney tissue of female rats and their progeny: biochemical and histopathological studies. Journal of physiology and biochemistry, 67(3), 307-316.

49. **Erin N, Afacan B, Ersoy Y, Ercan F, Balcı MK. (2008):** Gibberellic acid, a plant growth regulator, increases mast cell recruitment and alters Substance P levels. Toxicology, 254(1-2), 75-81.

50. **Sakr SA, El-Messedy FA, Abdel-Samei HA. (2002):** Histopathological and histochemical effects of gibberellin A3 on the kidney of albino rats. JOURNAL-EGYPTIAN GERMAN SOCIETY OF ZOOLOGY, 38(C), 1-10.